Detection and Distinction of Conductive and Magnetic Security Markers Using Eddy-Current Inspection

doi: 10.3379/msjmag.1605R002

Detection and Distinction of Conductive and Magnetic Security Markers Using Eddy-Current Inspection

T. Minamitani, S.Yamada
Institute of Nature and Environmental Technology, Kanazawa University, *Kakuma-machi, 9201192, Japan*

A printed magnetic marker is used effectively on bills or check for security. In securing of valuable documents, a further improvement in the degree of security is always indispensable. The addition of a conductive marker as well as a magnetic marker enhances the value of information and the reliability of these markers. We applied an eddy-current testing (ECT) technique by using the micro ECT probe with a giant magneto-resistance element (GMR) to detect both markers. Two markers can be detected and also distinguished by recognizing both the amplitude and phase of the ECT signal. This paper describes the method of detection and the results for these markers printed by a magnetic and conductive ink.

Keywords : Eddy-current inspection, GMR sensor, security, conductive marker, magnetic marker, discrimination.

1. Introduction

The magnetic apparatus for security identification uses a semiconductor magnetic resistance element or a pick-up coil as a magnetic detector. The apparatus detects the magnetic-ink marker or magnetic thread security identifier on a bill or check, and recognizes the truth or falsehood of the identifier. The conductive ink that includes nano-particles was developed recently and is easy to print out on a paper medium using an ink-jet printer similar to that of a magnetic ink [1]. The simultaneous detection and identification of both markers will contribute to an increase in security.

The authors developed an inspection process for printed circuit board traces using an eddy-current testing (ECT) probe with a giant magneto-resistance element (GMR). It enables us to detect disconnections and chipping errors on a high-density printed circuit board [2)~7)]. The ECT probe consists of a meander exciting coil excited by a few MHz current and a GMR sensor that is a few μm in width. The defects on a printed trace with a hundred μm width could be inspected. The probe can detect the magnetic field distribution near magnetic trace with the same size.

The paper describes that the proposed ECT probe can detect and discriminate both magnetic and conductive markers. The detection principle depends on the construction and characteristics of the ECT probe with GMR sensor and exciting coil [2),3)]. The difference of the ECT signals between two markers is described using a numerical analysis and experimental results.

2. Measurement of Markers

2.1 Signal of magnetic and conductive markers by ECT

Figs. 1(a) and (b) show the principle and difference between detecting conductive and magnetic markers using ECT technique [8), 9)]. Two kinds of markers are located vertically and are subjected to uniform AC exciting fields. In a conductive marker, eddy currents flow around the marker, and a penetrated magnetic flux can't penetrate into the marker. On the other hand, external magnetic fields are concentrated near a magnetic marker. When a scanned GMR sensor has sensitivity in the positive x-direction, the x-direction component B_x of magnetic fields near the point P1 has the difference distribution between conductive and magnetic markers as shown in Fig. 1. The phase of the detecting signal between the two markers becomes opposite in the presence of an AC exciting signal. When a GMR sensor is scanned across a marker, the phenomenon at the edge P1 also occurs at the edge P3 of the marker definitely and the phase is reversed. The x-component B_x of the magnetic fields disappears at the center P2 of the marker.

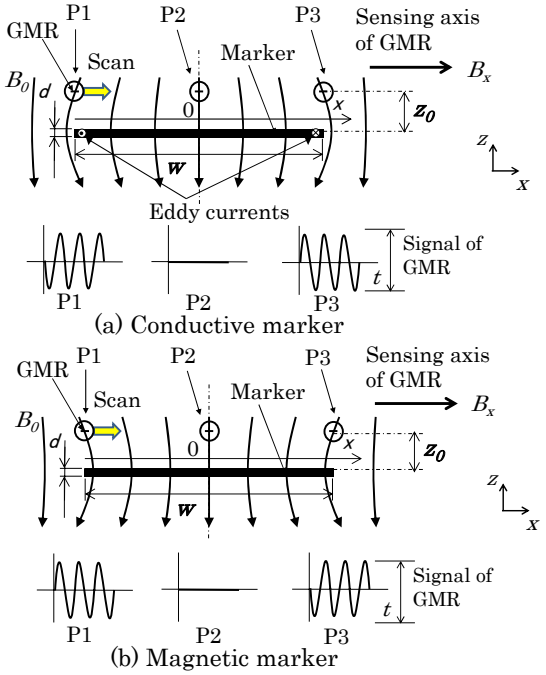

Fig. 1 Differences of AC magnetic fields near the edge of the markers.

It is assumed that the extension of the marker in the y-direction is long and a uniform external AC magnetic field $\mu_0 H_0$ (=B_0, z-component only) is applied to the marker in a vertical direction. A GMR sensor is installed to extract only the x component of the magnetic fields up only. The output voltage of a GMR with an angular frequency ω is,

$$V(x,t) \propto B_x(x) \sin(\omega t + \phi), \quad (1)$$

where $B_x(x)$ is the amplitude of the magnetic flux density at z_0 on a marker strip and ϕ is the phase shift with respect to the external applied fields.

For a magnetic marker (conductivity σ = 0), an external magnetic field is concentrated on a marker in Fig. 1(b) and the phase ϕ in Eq. (1) is given by

$$\phi = 0 \ (x < 0), \quad \phi = -\pi \ (x > 0). \quad (2)$$

For a conductive marker (permeability μ^* = 1), the phase of the magnetic flux density affected by eddy currents is shifted depending on the conductivity and shape of a marker. We assume an equivalent eddy-current circuit with magneto-motive force, equivalent resistance R_e, and inductance L_e [10]. An equivalent eddy current $i_e(t)$ is,

$$i_e(t) \propto \{\omega B_0 / (R_e^2 + (\omega L_e)^2)^{1/2}\} \sin(\omega t + \pi/2 - \theta_0), \quad (3)$$

where

$$\tan\theta_0 = \omega L_e / R_e. \quad (4)$$

For a conductive marker, magnetic fields near a marker are restrained by eddy currents and the x-component of the magnetic flux density is given by

$$\phi = -\pi \ (x < 0), \quad \phi = 0 \quad (x > 0). \quad (5)$$

According to Eqs. (4) and (5), the output voltage is expressed as,

$$V(x,t) \propto B_x(x) \sin(\omega t + \pi/2 - \theta_0 + \phi). \quad (6)$$

If a conductive marker has low conductivity and the condition ($\omega L_e << R_e$) is satisfied, the phase θ_0 is 0. The phase of the output voltage is then shifted from -π/2 to π/2 at x = 0 when scanning the sensor in the x-direction. For the marker with high conductivity ($\omega L_e >> R_e$), the phase is from -π to 0. For a prescribed value of conductivity, the phase is considered to be the mean of the both values. The phase change experienced during an x-direction scan of the sensor is summarized in Table 1. The phase movements of the conductive and magnetic markers are reversed with respect to each other.

Fig. 2 shows the amplitudes of both markers including phase signal. When the pick-up sensor is close to the edge of the marker at the positions, P1 and P3, the signal becomes the maximum and minimum peak value respectively. The signal vanishes at the position P2. The output waveform of the magnetic marker has a reversed pattern compared to the conductive marker.

Table 1 Phase of sensor signal to external magnetic fields.

Material of marker	Condition	Position of sensor	
		x < 0	x > 0
Magnetic	$\mu^* > 1, R_e = \infty$	0	−π
Conductive	$\omega L_e << R_e$	−π/2	π/2
	$\omega L_e >> R_e$	−π	0

2.2 Analysis of magnetic fields near markers

Fig. 2 shows the qualitative signal patterns for two kinds of markers. The waveform of magnetic fields depends on the exciting frequency, the material properties (conductivity and permeability), and the shape of the marker. The magnetic fields were calculated by using a 2D FEM. The simulated model and the sensing position are shown in Fig. 3. The marker was located under the uniform magnetic field with only a z-component (B_0 = 1 mT, f = 5 MHz). We simulated the amplitude of the x-component $B_x(x)$ and the phase with respect to the applied magnetic fields at z_0 = 0.3 mm on the surface of a marker.

We considered the marker models with different properties and a shape of w = 2, d = 0.05 mm. Fig. 4 shows the amplitude and phase of the magnetic flux density B_x. A solid line shows the amplitude of magnetic flux density, and a broken line is the phase with respect to the applied external fields at the edges, P1 and P3, of

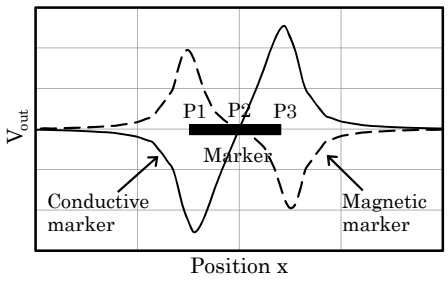

Fig. 2 Magnitude of B_x signal considering phase.

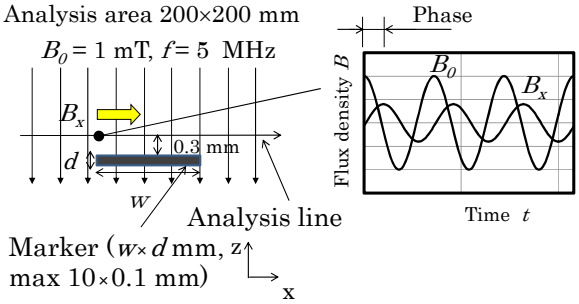

Fig. 3 Model of 2D FEM analysis.

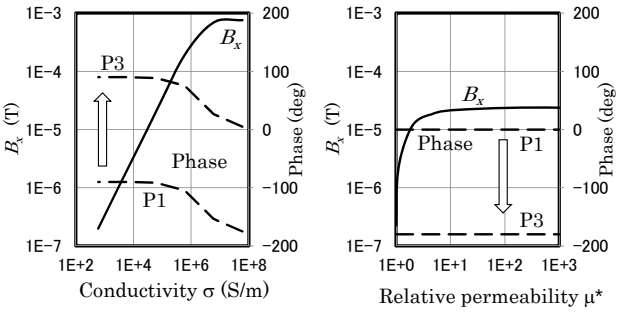

(a) Conductive marker (b) Magnetic marker

Fig. 4 Amplitude and phase of magnetic flux density vs. conductivity and permeability.

the marker. The magnetic flux density increases with increasing conductivity of a conductive marker. The phase changes by keeping the phase difference of π between the positions, P1 and P2. A magnetic shielding effect by eddy currents at a high conductivity shifts the phase to π/2 with increasing conductivity. On the contrary, as permeability rises in the case of a magnetic marker, the magnetic flux density increases, and the phase is constant.

Fig. 5 shows the amplitude and phase of magnetic flux density for different materials. Figs. 5(a) and (c) show the simulation results for the markers printed using conductive and magnetic ink. For comparison, the result for a metallic marker (Cu) with high conductivity is shown in Fig. 5(b). These results show that the amplitude of magnetic flux density has a peak at both edges of a marker, and the order of amplitude from highest to lowest becomes metal, a conductive ink, and magnetic ink marker. When a sensor passes by these markers, the change of phase signal is remarkably different between conductive and magnetic markers. The result suggests that the discrimination between both markers is possible because of the different behaviors of a phase.

Figs. 6 and 7 show the simulation results for amplitude and phase of magnetic flux density for three typical materials. When a marker shape becomes wide and thick, the magnetic flux density of all markers tends to increase. There is a little difference in the magnetic flux density as the thickness changes under the condition, $w >> d$.

For a conductive-ink marker, the condition ($\omega L_e << R_e$) in Table 1 is satisfied, thus the phase is shifted from -π/2 to π/2 between the positions, P1 and P3. As the

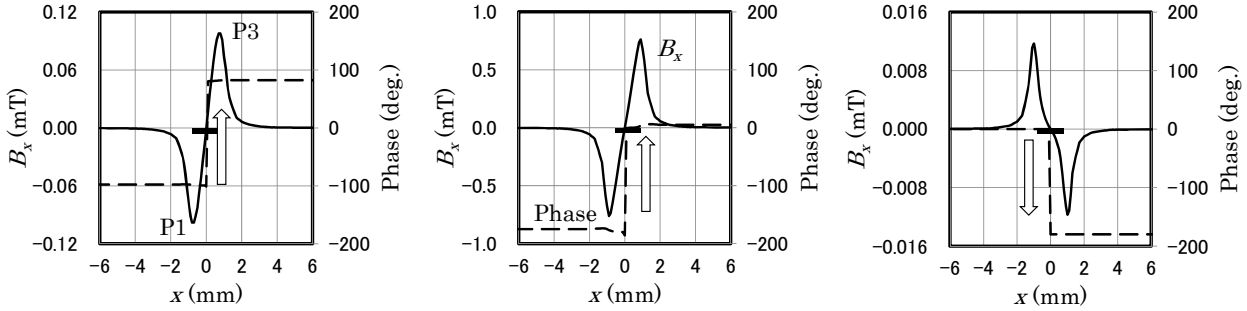

(a) Conductive ink (μ^*= 1, σ= 3×10^5 S/m) (b) Metal (μ^*= 1, σ= 6×10^7 S/m) (c) Magnetic ink (μ^*= 10, σ = 0)

Fig. 5 Signal patterns of magnetic flux density for markers with different materials.

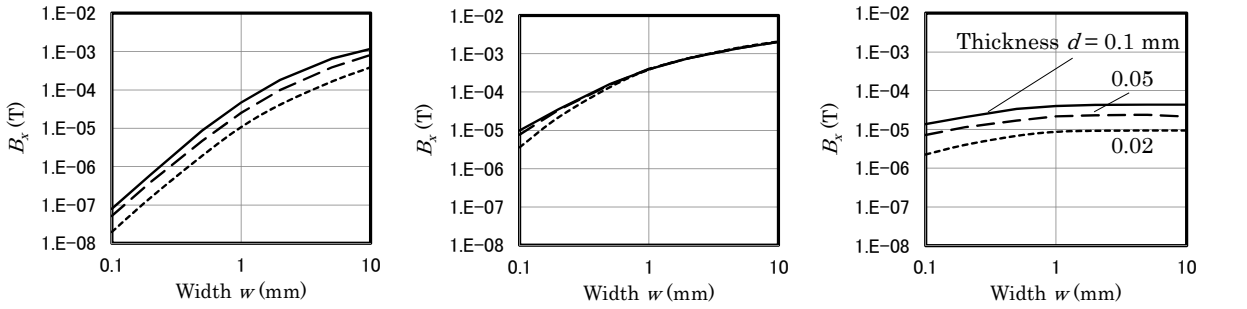

(a) Conductive ink (μ^*= 1, σ= 3×10^5 S/m) (b) Metal (μ^*= 1, σ= 6×10^7 S/m) (c) Magnetic ink (μ^*=10, σ = 0)

Fig. 6 Amplitude of magnetic flux density as a function of width and thickness of markers.

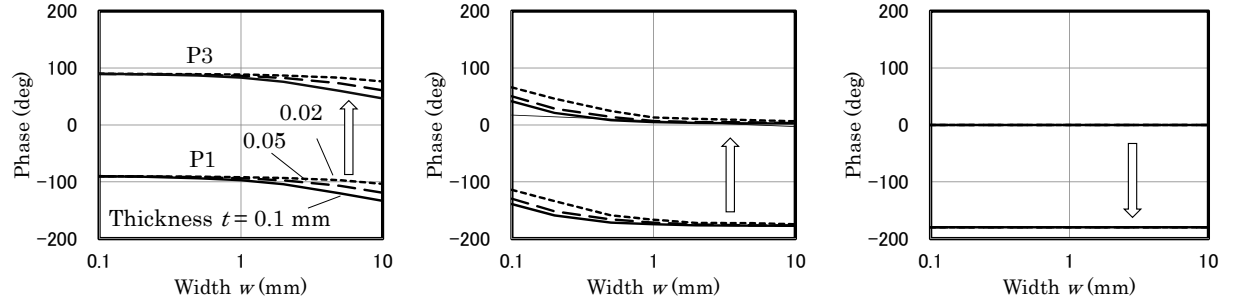

(a) Conductive ink (μ^*= 1, σ = 3×10^5 S/m) (b) Metal (μ^*= 1, σ = 6×10^7 S/m) (c) Magnetic ink (μ^*= 10, σ = 0)

Fig. 7 Phase of magnetic flux density as a function of width and thickness of markers.

width increases, the phase characteristics change a little. On the contrary, the condition ($\omega L_e >> R_e$) in Table 1 is satisfied for a metal marker with high conductivity.

According to these results, we concluded that two kinds of markers can be distinguished by recognizing both amplitude and phase of the ECT signal.

3. Experimental Measurement of Markers

3.1 Experimental apparatus

Fig. 8 shows the outline of the testing equipment with the ECT probe. The ECT probe has an exciting coil with a meander structure and dimensions of 0.2, 10, and 0.035 mm in width, length, and thickness respectively.

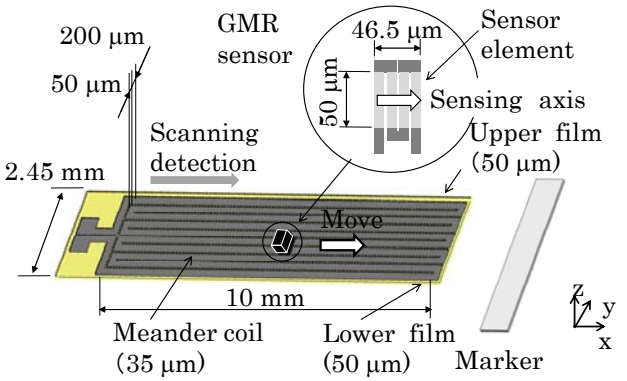

Fig. 8 Structure of ECT probe.

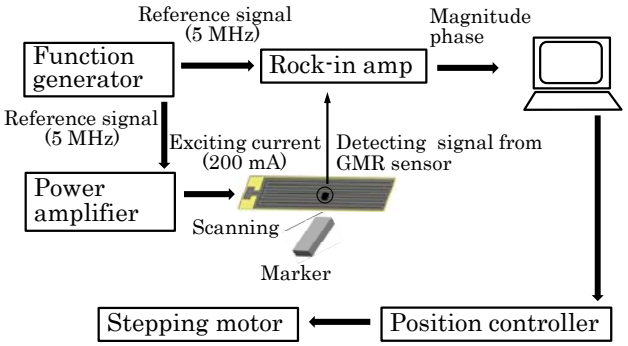

Fig. 9 Measurement system.

The pick-up element is giant magneto-resistance sensor with footprint 50×50 μm. The meander coil induces x-direction eddy currents along the trace of meander coil on a testing object. The GMR sensor detects the x-direction magnetic fields parallel to the induced eddy currents. When the probe is scanned orthogonal to a strip marker, the signal appears near both edges of the markers.

The block diagram of the measuring system for the ECT signal is shown in Fig. 9. There are three blocks, consisting of a high frequency generator and power amplifier for the exciting coil, xy-stage for scanning probe, and digital phase detector for the ECT signal. The reference signal of the phase detector is the exciting current. The amplitude and phase of the ECT signal are then detected.

3.2 Experimental results of different marker materials

Fig. 10 shows the amplitude of the ECT signals including phase for the following kinds of markers, conductive-ink, metallic, and magnetic-ink marker. The metallic marker is made of copper film. The conductivity of the conductive-ink marker depends on the printing condition. The value of conductivity for the printed conductive marker was 2×10^6 S/m experimentally derived by 4-point probe method and is about 3 % of the value for copper. The magnitude of the output voltage from lowest to highest for the given materials is in the following order metal, conductive ink, and magnetic ink. The pattern of the signal is similar to the simulated one shown in Fig. 5. We can recognize the definite difference of the pattern between conductive and magnetic markers from the experimental results.

Figs. 11 and 12 show the experimental results for amplitude and phase shift of the ECT signal on the markers with a 50 μm thickness and the widths from 1.0 to 10 mm. When the width of a marker becomes narrow, the output voltage of the signal tends to decrease. The phase shifts by about -π for a conductive marker and by +π for magnetic marker. These results confirm that the detection of a phase change enables us to distinguish between a magnetic-ink and conductive-ink marker. The possibility of distinguishing between two kinds of markers was confirmed also by experiments.

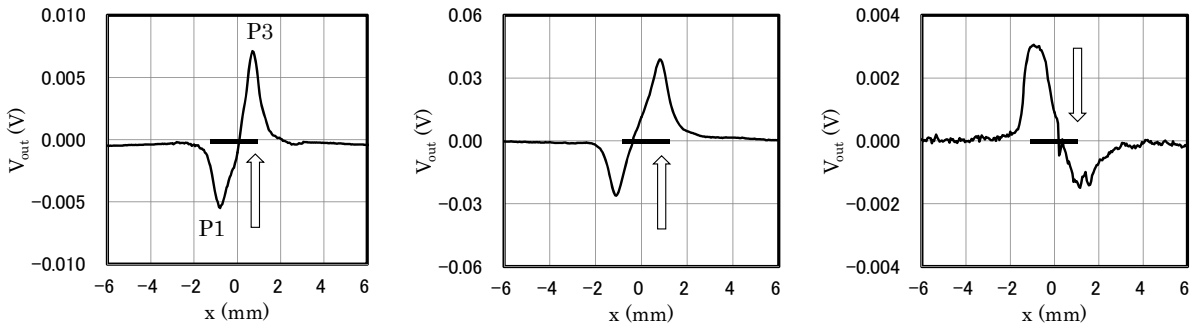

(a) Conductive ink (μ^*= 1, σ= 2×10^6 S/m) (b) Metal (μ^*= 1, σ= 6×10^7 S/m) (c) Magnetic ink (μ^*= 1.05, σ = 0)

Fig. 10 Signal patterns of ECT signals for markers with different materials.

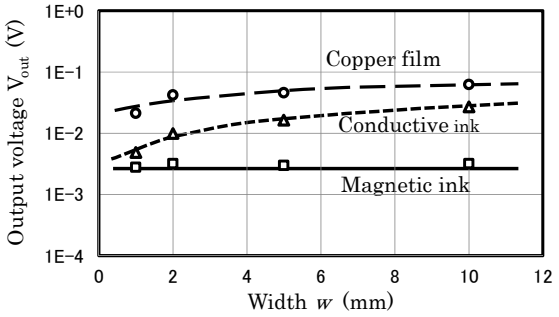

Fig. 11 Amplitudes of signal vs. width of markers with different materials.

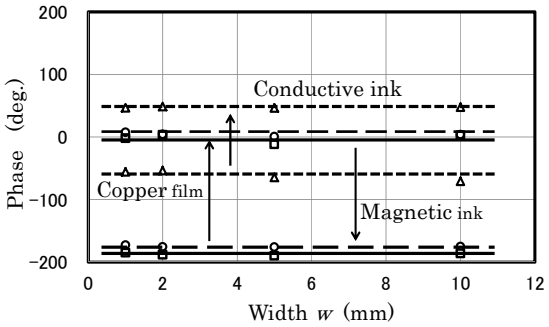

Fig. 12 Phase shift vs. width of markers with different materials.

4. Conclusions

The μ-ECT probe using GMR sensor enabled us to detect and distinguish between markers printed by conductive and magnetic inks. The feature of detecting signal was discussed among two kinds of markers and the difference in the phase was important from the distinction of markers. We built the experimental apparatus using the probe and confirmed experimentally that it was possible to classify two kinds of markers by the phase of pick-up signal.

Even if the visual appearance such as color and shape of a marker are the same, it is possible to detect and distinguish conductive and magnetic markers by their electromagnetic properties. The simultaneous use of two kinds of markers dramatically improves the reliability of marker security printed on a paper medium because of increased information.

Acknowledgements This work was supported in part by a Grant-in-Aid for Scientific Research (C) 26420384 from the Ministry of Education, Culture, Sports, Science, and Technology in Japan.

References

1) AgIC Inc., http://agic.cc/ja/ (2015).
2) S. Yamada, K. Chomusuwan, Y. Fukuda, M. Iwahara,H. Wakiwaka, and S. Shoji, *IEEE Trans. on Magn.*, **40**, 4 (2004).
3) K. Chomusuwan, Y. Fukuda, S. Yamada, M. Iwahara, H. Wakiwaka, and S. Shoji, *J. Magn. Soc. JPN*, **4**, 1 (2004).
4) M. Cacciola, G. Megalo, D. Pelicano, and F.C. Morabino, *Sensors and Actuators A : Physical*, **167**, 1, 25 (2011).
5) K. Chomusuwan, S. Yamada, and M. Iwahara, *IEEE Sensors J.,* **7**, 5 (2007).
6) K. Chomusuwan, S. Yamada, and M. Iwahara, *IEEE Trans. on Magn.*, **43**, 6 (2007).
7) H. Murata, Y. Ikehata, and S. Yamada, *IEEJ Trans. on Electronics Information and System*, **134**, 5 (2014). [in Japanese]
8) T. Minamitani, S. Uraoka, and S. Yamada, *Digest of 2015 JIEE Annual Conference*, **2-115** (2015). [in Japanese]
9) T. Minamitani, S. Uraoka, and S. Yamada, *JIEE Technical Paper of Magnetic Meeting,* **MAG-14-139** (2014). [in Japanese]
10) R.L.Stoll, The analysis of eddy currents, Chp.2, Clarendon Press, Oxford (1974).

Received Nov.19, 2015; Revised Jan.07, 2016; Accepted Feb.20, 2016